ORIGINAL ARTICLE

WILEY **Cancer Science**

Increased nicotinamide adenine dinucleotide pool promotes colon cancer progression by suppressing reactive oxygen species level

Sun M. Hong[1] | Sung W. Hwang[2] | Taejun Wang[3] | Chang W. Park[4] | Yeon-Mi Ryu[5] | Jin-Hak Jung[5] | Ji H. Shin[6] | Sang-Yeob Kim[5,7] | Jong L. Lee[8] | Chan W. Kim[8] | Gyesoon Yoon[1] | Ki H. Kim[3,9] | Seung-Jae Myung[2,5,7] | Kwan Y. Choi[3] 🆔

[1]Department of Biochemistry and Department of Biomedical Sciences (BK21 Plus), Ajou University School of Medicine, Suwon, Korea

[2]Department of Gastroenterology, Asan Medical Center, University of Ulsan College of Medicine, Seoul, Korea

[3]Division of Integrative Biosciences and Biotechnology, Pohang University of Science and Technology (POSTECH), Pohang, Korea

[4]Biokogen Inc. F255, Korea National Food Cluster, Iksan, Jeonbuk, Korea

[5]Asan Institute for Life Sciences, Asan Medical Center, Seoul, Korea

[6]Department of Life Sciences, Pohang University of Science and Technology (POSTECH), Pohang, Korea

[7]Department of Convergence Medicine, University of Ulsan College of Medicine, Seoul, Korea

[8]Department of Colon and Rectal Surgery, Asan Medical Center, University of Ulsan College of Medicine, Seoul, Korea

[9]Department of Mechanical Engineering, Pohang University of Science and Technology (POSTECH), Pohang, Korea

Correspondence
Kwan Y. Choi and Ki H. Kim, Division of Integrative Biosciences and Biotechnology, Pohang University of Science and Technology, Nam-gu, Pohang, Korea.
Emails: kwanychoi@gmail.com and kiheankim@postech.ac.kr
and
Seung-Jae Myung, Department of Gastroenterology, Asan Medical Center, University of Ulsan College of Medicine, Songpa-gu, Seoul, Korea.
Email: sjmyung@amc.seoul.kr

Nicotinamide adenine dinucleotide (NAD) exists in an oxidized form (NAD^+) and a reduced form (NADH). NAD^+ plays crucial roles in cancer metabolism, including in cellular signaling, energy production and redox regulation. However, it remains unclear whether NAD(H) pool size (NAD^+ and NADH) could be used as biomarker for colon cancer progression. Here, we showed that the NAD(H) pool size and NAD^+/NADH ratio both increased during colorectal cancer (CRC) progression due to activation of the NAD^+ salvage pathway mediated by nicotinamide phosphoribosyltransferase (NAMPT). The NAMPT expression was upregulated in adenoma and adenocarcinoma tissues from CRC patients. The NADH fluorescence intensity measured by two-photon excitation fluorescence (TPEF) microscopy was consistently increased in CRC cell lines, azoxymethane/dextran sodium sulfate (AOM/DSS)-induced CRC tissues and tumor tissues from CRC patients. The increases in the NAD(H) pool inhibited the accumulation of excessive reactive oxygen species (ROS) levels and FK866, a specific inhibitor of NAMPT, treatment decreased the CRC nodule size by increasing ROS levels in AOM/DSS mice. Collectively, our results suggest that NAMPT-mediated upregulation of the NAD(H) pool protects cancer cells against detrimental oxidative stress and that detecting NADH fluorescence by TPEF microscopy could be a potential method for monitoring CRC progression.

KEYWORDS
colon cancer, inflammation, NAD(H) pool, nicotinamide phosphoribosyltransferase, two-photon excitation fluorescence microscopy

Hong and Hwang equally contributed to this work.

-----

1 | INTRODUCTION

Worldwide, colorectal cancer (CRC) is the third most common cancer diagnosed in men and the second most common in women. It also has the fourth highest cancer mortality rate in men and the third highest in women.[1] The vast majority of CRC cases are linked to environmental causes, such as diet, exercise, weight, food-borne mutagens, specific intestinal commensals and chronic intestinal inflammation.[2] For example, patients with inflammatory bowel disease, such as ulcerative colitis or Crohn's disease, are 5 to 7 times more likely to develop CRC.[3-6] In addition to cancer cells, tumors are composed of various immune and inflammatory cells, including macrophages, neutrophils and T lymphocytes. These cells can influence cancer cells via the production of cytokines, chemokines, growth factors and reactive oxygen species (ROS).[7] ROS cause DNA damage, resulting in an accumulation of gene mutations, and activate specific signaling pathways that promote tumor development.[8] However, if ROS levels increase over a certain threshold that is unfavorable for cellular survival, they may induce cytotoxicity and limit cancer progression.[9] Cancer cells should survive under metabolic stress conditions, such as nutrient deprivation, hypoxia and inflammation, which lead to the accumulation of excessive ROS levels during cancer progression.[10] For cancer to progress under such circumstances, cancer cells must acquire adaptive mechanisms for protection against the potential toxic effects induced by elevated ROS levels.

Nicotinamide adenine dinucleotide (NAD) is a critical coenzyme that exists in both oxidized (NAD^+) and reduced (NADH) forms. In mammals, NAD^+ is biosynthesized via 2 major pathways: the de novo and salvage pathways.[11] The salvage pathway is important for the maintenance of NAD^+ levels in cancer cells and works via 2 major pathways, one using nicotinamide phosphoribosyltransferase (NAMPT) and the other using nicotinate phosphoribosyltransferase (NAPRT). NAMPT acts as a rate-limiting enzyme in the salvage pathway and works by transferring a phosphoribosyl group to nicotinamide (NAM) to form nicotinamide mononucleotide (NMN). NMN is then converted into NAD^+ by nicotinamide mononucleotide adenylyltransferase (NMNAT). NAPRT is involved in the synthesis of NAD^+ from nicotinic acid.[12] NAMPT is upregulated in various cancer types, including prostate, breast, colorectal, gastric and liver cancers,[13] and could be induced in response to stressors such as genotoxic stress and nutrient deprivation.[14] FK866, a specific inhibitor of NAMPT, has been reported to inhibit breast cancer progression in a xenograft model,[15] and colon cancer progression in an inflammation-induced model.[16] Cancer cells are reported to have a high rate of NAD^+ turnover and a low ratio of cytosolic NAD^+/NADH due to their elevated metabolic needs.[12] Therefore, it remains to be resolved whether the NAD^+/NADH ratio and the NAD(H) pool size can regulate cancer progression and the underlying mechanism.

Because NADH is autofluorescent, it can be utilized in nondestructive optical imaging techniques without the use of exogenous labeling agents. Indeed, the redox ratio, which is the fluorescence intensity ratio of NADH and FAD (NADH/FAD), is commonly used in optical metabolic imaging methods. Previous studies demonstrated that the redox ratio was increased in human papillomavirus-transformed cells and estrogen receptor-positive breast cancer cell lines.[17,18] Two-photon excitation fluorescence (TPEF) microscopy is well suited for high-resolution, 3-dimensional, non-invasive measurements of deep regions within living tissue.[19,20] The detection of NADH by TPEF microscopy during CRC progression in a non-invasive manner would be important for developing not only a diagnostic biomarker but also therapeutics targets associated with NAD^+ pathways.

In the present study, we investigated the correlation between the NAD(H) pool size and CRC progression and evaluated NADH as a potential prognostic marker. The NAD(H) pool size was increased during colon cancer progression by activating the salvage pathway of NAD^+ synthesis and could protect tumor cells from excessive oxidative stress induced by inflammation. NADH fluorescence intensity, as measured by TPEF microscopy, was consistently elevated in tumor tissues from CRC patients, suggesting that NADH fluorescence intensity could be a biomarker for CRC progression.

2 | MATERIALS AND METHODS

More detailed descriptions of cell culture, drug treatments, western blot analysis, immunohistochemistry, immunofluorescence, stable gene knockdown, gene silencing with siRNA, NAD^+/NADH and $NADP^+$/NADPH assay, two-photon excitation fluorescence imaging, redox analysis and RT-PCR are provided in the supporting information (Appendix S1).

2.1 | Azoxymethane/dextran sodium sulfate tumor model

C57BL/6J mice (6 weeks old) were i.p. injected with 10 mg/kg azoxymethane (AOM) (A5486, Sigma Aldrich, St Louis, MO, USA). After 7 days, the mice were administered 2 cycles of 2% DSS (160110, MP Biomedical, Solon, OH, Canada) for 7 days. The mice were killed 60 days after the cessation of DSS treatment. The colons of those mice were dissected longitudinally and washed with PBS immediately after sacrifice. The colonic tissues were laid down with the mucosa layer facing up on microscope slides for TPEF imaging.

2.2 | Reactive oxygen species assay

After 24 h of H_2O_2 treatment, carboxy-H2DCFDA (Invitrogen, Carlsbad, CA, USA) was added to each dish at a concentration of 20 μmol/L for 30 minutes. The cells were incubated for 45 minutes with medium, and the fluorescence levels were determined using a microplate reader (Tecan, Grödig, Austria). To detect ROS levels in mouse tissues, carboxy-H_2DCFDA (Invitrogen) was added to colon tissues at a concentration of 20 μmol/L and incubated for 15 minutes. The tissues were washed with PBS. The fluorescence was

detected at 950 nm excitation by two-photon microscopy (TCS SP5 II, Leica, Wetzlar, Germany).

2.3 | Statistical analysis

Statistical analyses were performed using a 2-tailed Student's t test. $P < .05$ was considered statistically significant. All samples except for animal samples were prepared in triplicate for every experiment. The data represent at least 3 independent experiments and are presented as the mean ± SD.

2.4 | Study approval

Human colon cancer specimens and their paired normal specimens were obtained from Asan Bio-Resource Center. All processes were performed under the approval of the Asan Medical Center Institutional Review Board. All animal experiments were performed in accordance with the guidelines and regulations and with the approval of The Institutional Animal Care and Use Committees at POSTECH.

3 | RESULTS

3.1 | The NAD(H) pool size could increase in malignant colorectal cancer cell lines resulting from activation of the salvage pathway of NAD⁺ synthesis

As cancer cells require the rapid turnover of NAD⁺,[12] we investigated the correlation of NAD(H) pool size and NAD⁺/NADH ratio with colon cancer progression. We measured each level of NAD+ and NADH in normal gut epithelial CCD-18Co cells and in CRC cell lines, including the SW480, RKO and HCT116 cell lines by enzymatic method. We obtained NAD(H) pool size by adding levels of NAD⁺ and NADH and the ratio of NAD⁺/NADH. The NAD(H) pool was
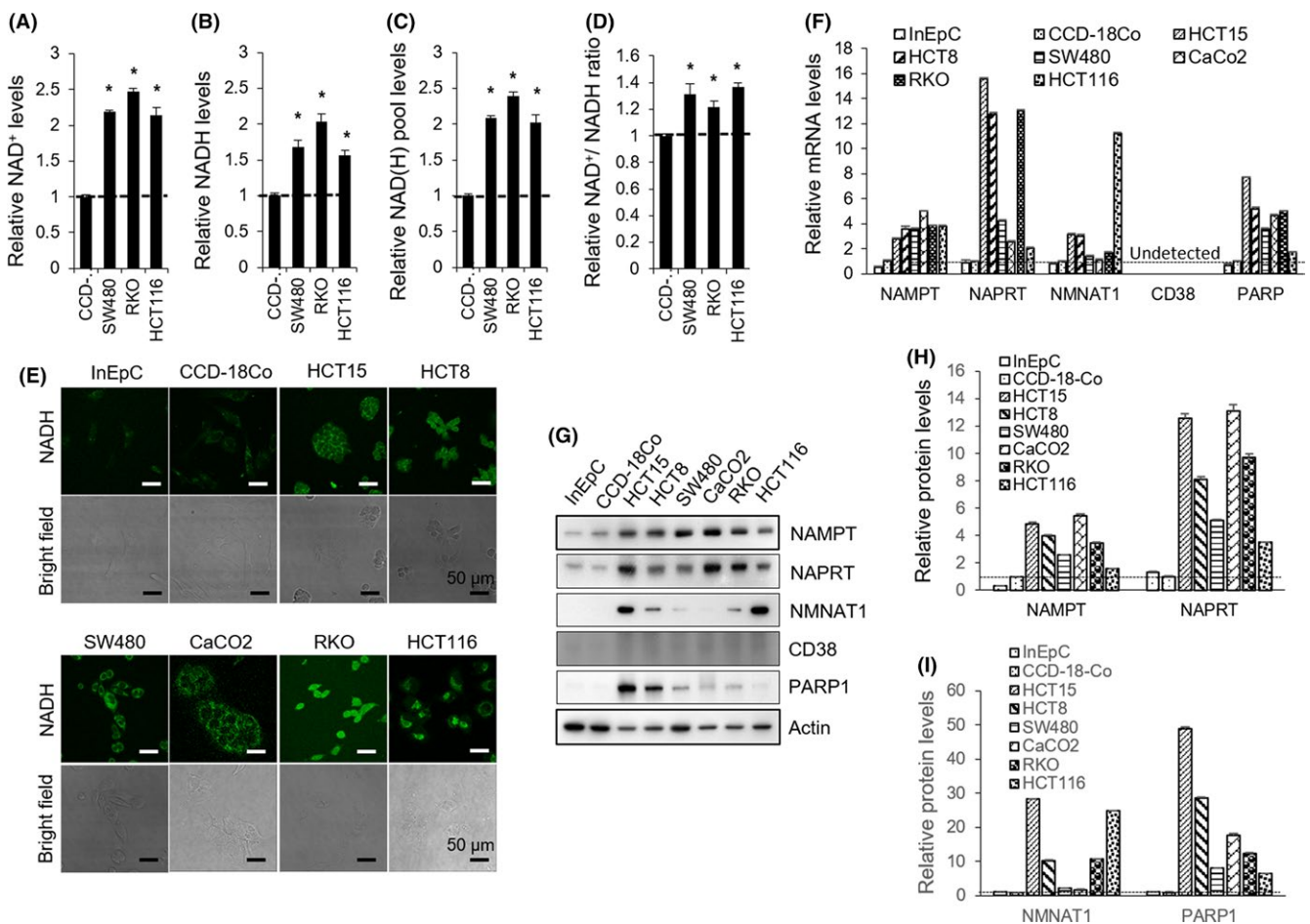

FIGURE 1 The NAD⁺ salvage pathway was activated, and the NAD(H) pool size was increased in malignant colorectal cancer (CRC) cell lines. A, B, Levels of NAD⁺ and NADH were quantified in normal gut epithelial cells (CCD-18Co) and CRC cell lines (SW480, RKO and HCT116). C, NAD⁺/NADH ratios were measured in the indicated cells. D, The NAD(H) pool represented the sum of the NAD⁺ and NADH levels. E, NADH fluorescence was detected in gut epithelial cells and CRC cell lines by two-photon excitation fluorescence (TPEF) microscopy (scale bar, 50 μm). F, mRNA levels of nicotinamide phosphoribosyltransferase (NAMPT), nicotinate phosphoribosyltransferase (NAPRT), NMNAT1, CD38 and PARP were assessed by quantitative RT-PCR analysis. G, Protein levels were measured by western blotting using whole-cell lysates. H, I, Protein levels were analyzed by densitometry using the ImageJ software. The bars represent the mean ± SD (n = 9). *$P < .05$ by Student's t test

larger in the CRC cell lines than in normal gut epithelial cells due to the increase in both the NAD$^+$ and NADH levels (Figure 1A-C). The NAD$^+$/NADH ratio was also higher in the CRC cell lines (Figure 1D). In addition, NADH fluorescence detected using TPEF microscope at a 740-nm wavelength was consistently stronger in the CRC cell lines than in the normal gut epithelial cells, InEpC and CCD-18Co cells (Figure 1E). Therefore, CRC cells were found to maintain a large NAD(H) pool size and a high NAD$^+$/NADH ratio.

To identify which factors could increase the NAD(H) pool and NAD$^+$/NADH ratio in CRC cells, we examined the levels of enzymes that produced or consumed NAD$^+$. The mRNA and protein levels of enzymes in the salvage pathway of NAD$^+$ synthesis, such as NAMPT, NAPRT and NMNAT1, were upregulated in CRC cell lines relative to normal gut epithelial cells. However, those of enzymes consuming NAD$^+$, such as CD38 and PARP-1, were not

correlated with the sizes of the NAD(H) pool or ratios of NAD$^+$/NADH (Figure 1F-I), suggesting that activation of the salvage pathway could increase both the NAD(H) pool size and the NAD$^+$/NADH ratio in CRC cells.

3.2 | NADH fluorescence reflects the NAD(H) pool size

We next examined whether inhibition of the enzymes NAMPT, NAPRT and NMNAT1 could decrease NAD$^+$ and NADH levels. Knockdown of NAPRT or NMNAT1 barely reduced the NAD$^+$ and NADH levels, whereas knockdown of NAMPT significantly decreased both the NAD$^+$ (Figure 2A) and NADH (Figure 2B) levels, leading to a reduced NAD(H) pool (Figure 2C). The NAD$^+$/NADH ratio was also reduced by NAMPT knockdown (Figure 2D).
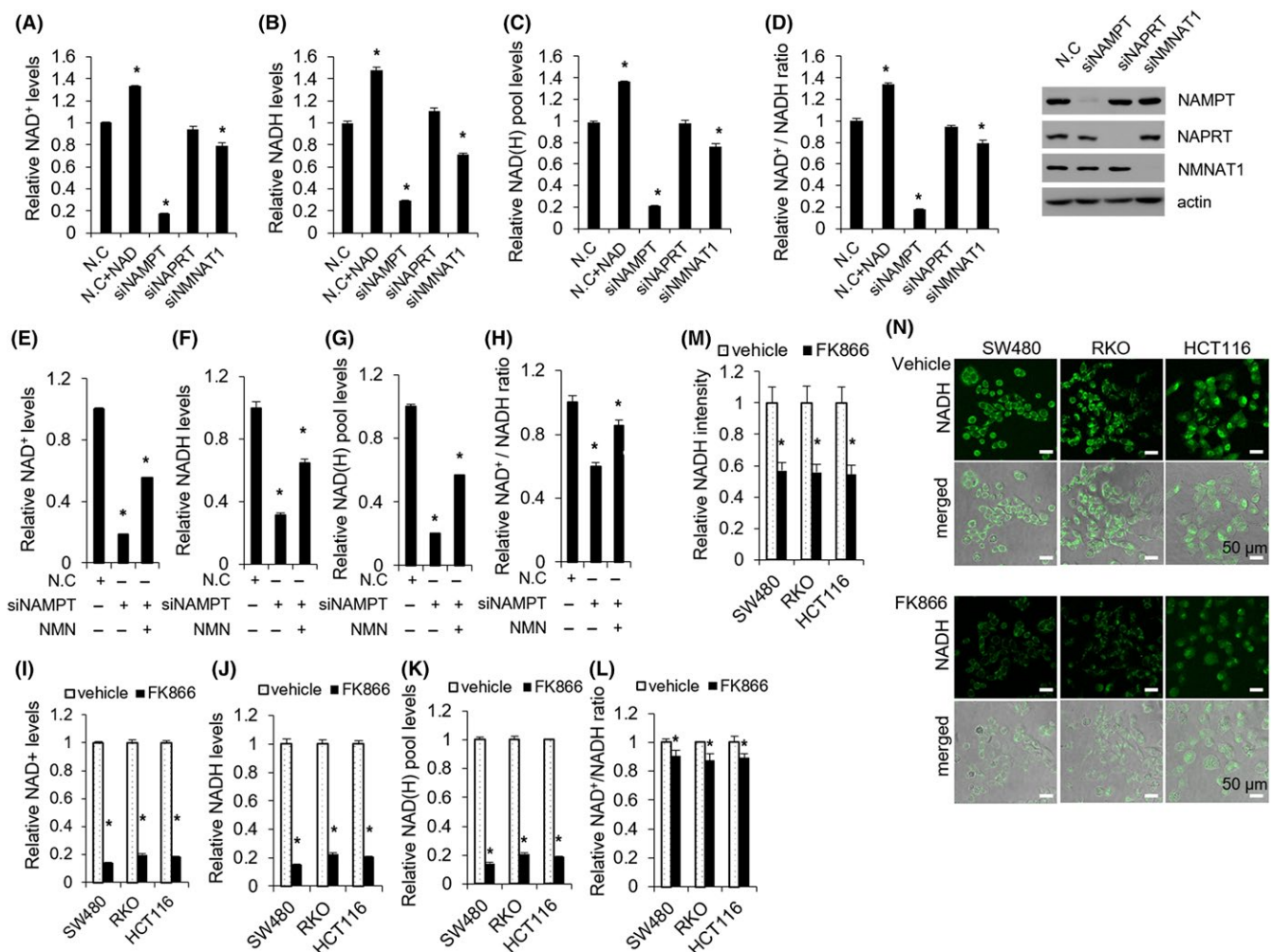

FIGURE 2 Nicotinamide phosphoribosyltransferase (NAMPT) inhibition reduced the NAD(H) pool size. A-D, Scrambled siRNA and siRNA targeting NAMPT, nicotinate phosphoribosyltransferase (NAPRT) or NMNAT1 were transfected into RKO cells for 60 h, followed by NAD$^+$ treatment for 12 h. Levels of NAD$^+$ and NADH were assessed, in addition to the NAD$^+$/NADH ratio. E-H, Scrambled siRNA or siRNA targeting NAMPT was transfected into RKO cells for 60 h, followed by NMN treatment for 12 h. Levels of NAD$^+$ and NADH as well as the NAD$^+$/NADH ratio were assessed. I-L, NAD$^+$ and NADH levels were measured following FK866 treatment for 24 h in colorectal cancer (CRC) cell lines. M, NADH fluorescence was detected by two-photon excitation fluorescence (TPEF) microscopy following FK866 treatment for 4 h in CRC cell lines (scale bar, 50 μm). N, NADH fluorescence intensity in individual cells was quantified using the MATLAB program. The bars represent the mean ± SD (n = 9). *P < .05 by Student's t test

Moreover, NMN treatment restored the levels of NAD^+, and NADH and increased the NAD(H) pool and NAD^+/NADH ratio in NAMPT-knockdown cells (Figure 2E-H), indicating that NAMPT could not only critically determine the NAD^+ levels but also the NAD(H) pool size.

Nicotinamide phosphoribosyltransferase inhibition through treatment with FK866 for 12 hours slightly decreased the NAD^+/NADH ratio (Figure 2L) but dramatically reduced the NAD^+ and NADH levels (Figure 2I,J), resulting in the depletion of the NAD(H) pool (Figure 2K). Consistently, the NADH fluorescence intensity was dramatically decreased in CRC cells following treatment with FK866

for 4 hours (Figure 2M,N), suggesting that the NADH fluorescence intensity using TPEF microscopy could be positively correlated with the NADH pool size.

Both NADH and NADPH can be excited at the same wavelength; therefore, we further investigated the influence of NADPH on the fluorescence intensity determined by TPEF microscopy at a 740-nm wavelength. For this purpose, we transfected siRNA specific to glucose-6-phosphate dehydrogenase (G6PD), an enzyme that is critical for NADPH production (Figure S1E). G6PD knockdown specifically downregulated NADPH levels (Figure S1A-D) and did not reduce the fluorescence intensity (Figure S1E,F).
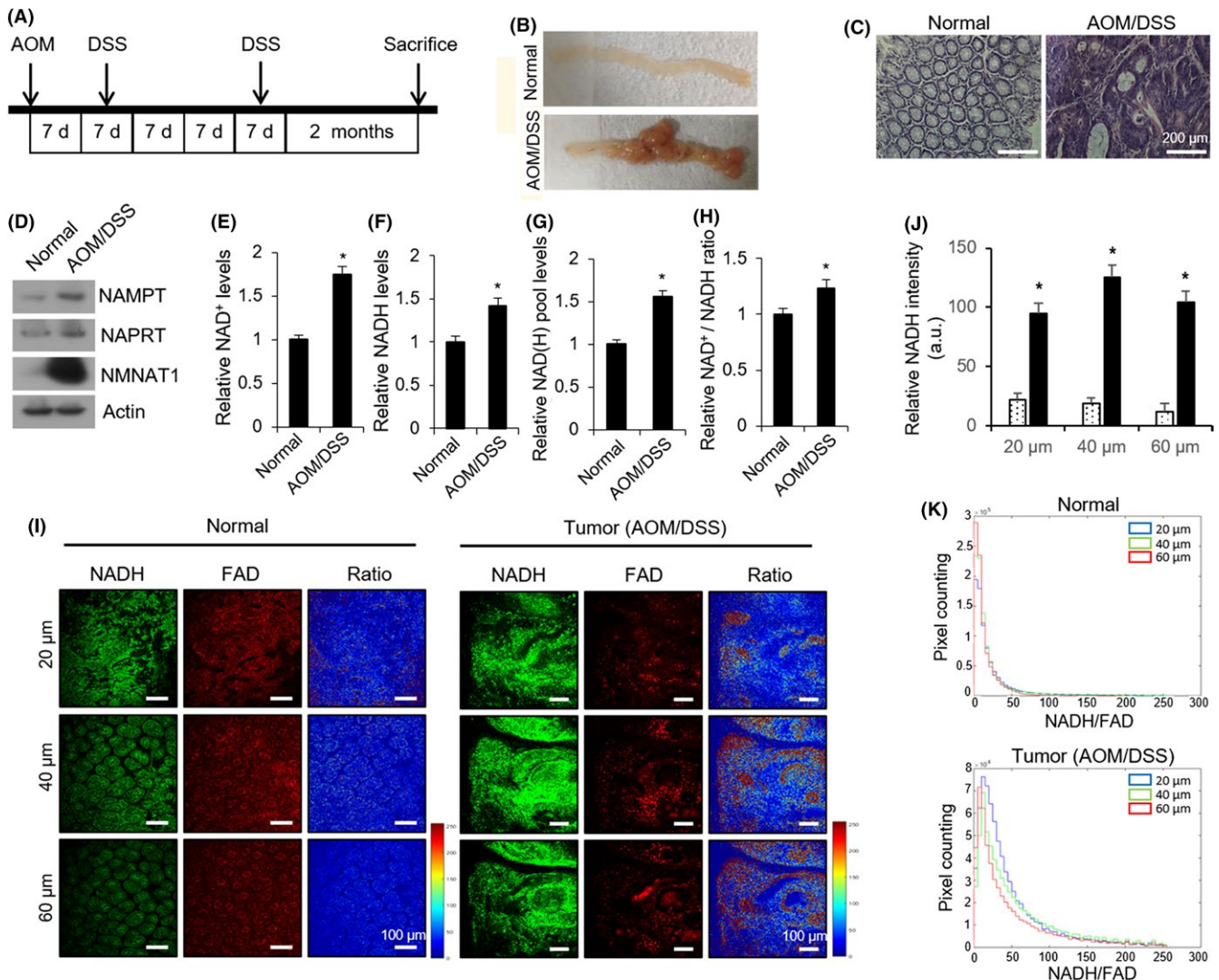

FIGURE 3 The NAD(H) pool size was increased in azoxymethane/dextran sodium sulfate (AOM/DSS)-induced colorectal cancer. A, Experimental scheme used to induce colorectal cancer (CRC) formation in C57BL/6 mice: after an initial injection of 10 mg/kg AOM, 2% DSS was administered via the drinking water, followed by normal drinking water. B, Representative images of excised mouse colon tissues. Mice were killed 2 mo after DSS treatment (n = 5 per time point). C, Tumor tissues were embedded in paraffin and sectioned (5 μm thick). The sections were stained with H&E (scale bar, 200 μm). D, Protein levels of nicotinamide phosphoribosyltransferase (NAMPT), nicotinate phosphoribosyltransferase (NAPRT) and NMNAT1 were assessed by western blotting of tissue lysates. E-H, Levels of NAD^+ and NADH were quantified in normal colon tissue and AOM/DSS-induced CRC tissue. The bars represent the mean ± SD (n = 5). *$P < .05$ by Student's t test. I, NADH and FAD fluorescence levels were detected in normal colon tissue and AOM/DSS-induced CRC tissue at the indicated depths of 20, 40 and 60 μm (scale bar, 100 μm). J, NADH fluorescence intensity at the indicated depth was quantified. *$P < .05$ by Student's t test. K, The NADH/FAD ratios in normal tissue and AOM/DSS-induced CRC tissue were quantified at the indicated depths using the MATLAB program

NAMPT knockdown led to a decrease in fluorescence intensity (Figure S1F,G). This result was likely because 2-fold more NADH was present than NADPH (Figure S1B,D). Our observations indicated that NAMPT could regulate the NAD(H) pool size by mediating NAD$^+$ influx and that the fluorescence intensity detected by TPEF microscopy at a 740-nm wavelength could reflect the NAMPT-mediated regulation of the NAD(H) pool size.

3.3 | The NAD(H) pool increases in azoxymethane/dextran sodium sulfate-induced colon cancer

The increased NAD(H) pools found in CRC cell lines prompted us to investigate whether the NAD(H) pool was also augmented in AOM/DSS mice, a model created by injecting C57BL/6J mice with a single dose of the carcinogen AOM, followed by 2 cycles of DSS administration (Figure 3A). Mice exposed to the AOM/DSS treatment regimen developed CRC (Figure 3B,C). The NAD$^+$ salvage pathway

was consistently activated in the AOM/DSS mice, as indicated by the overexpression of NAMPT, NAPRT and NMNAT1 (Figure 3D). As NAMPT was critical for the increased NAD(H) pool size (Figure 2), we further examined the types of cells that upregulated NAMPT in tumor tissues. NAMPT was entirely upregulated in colon cancer tissues, including colon cancer cells and immune cells. F4/80, a macrophage marker, and CD3, a T cell marker, were also increased in AOM/DSS-induced CRC tissues and co-localized with NAMPT (Figure S2). Next, we compared the NAD(H) pool size between the normal gut epithelium and AOM/DSS-induced tumor tissue. Both NAD$^+$ and NADH levels were markedly increased in AOM/DSS-induced tumor tissue (Figure 3E,F), leading to a 1.6-fold increase in the NAD(H) pool size (Figure 3G). The NAD$^+$/NADH ratio was also increased by 1.2-fold (Figure 3H). Consistent with the above results, the NADH fluorescence intensity and the redox ratio (NADH/FAD fluorescence) were also elevated in AOM/DSS-induced tumor tissue (Figure 3I-K). Our data indicated that the NAD(H) pool size increases
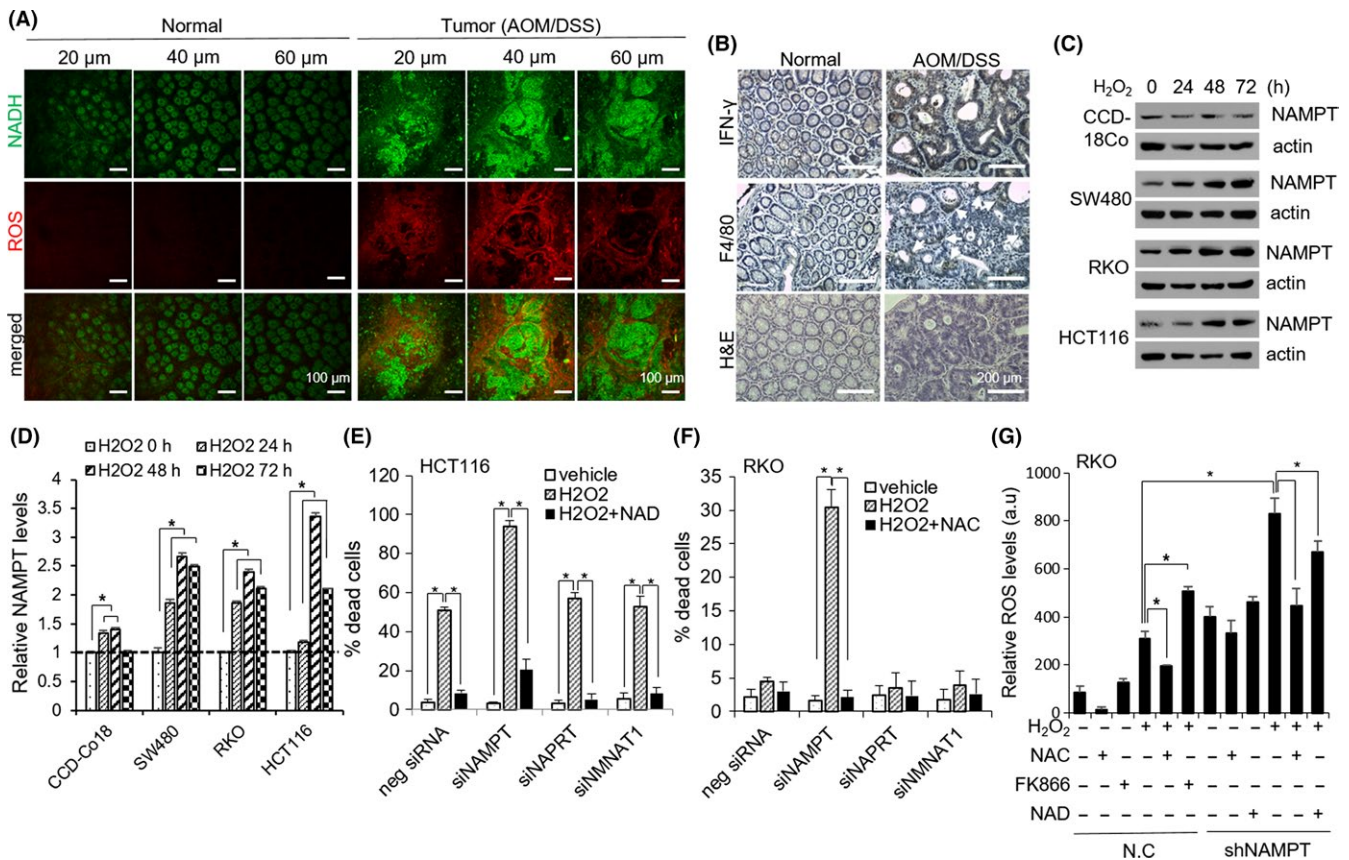

FIGURE 4 Nicotinamide phosphoribosyltransferase (NAMPT) expression was induced by inflammation-induced reactive oxygen species (ROS) production and protected colorectal cancer (CRC) cells from oxidative stress by increasing the NAD(H) pool size. A, In normal tissue and azoxymethane/dextran sodium sulfate (AOM/DSS)-induced colorectal cancer (CRC) tissue, NADH fluorescence was measured by two-photon excitation fluorescence (TPEF) microscopy. ROS levels were also determined by TPEF microscopy following incubation with carboxy-H$_2$DCFDA dye (scale bar, 100 μm). B, Tumor tissues were embedded in paraffin and sectioned (5-μm thick). The sections were stained with anti-F4/80 and anti-IFN-γ antibodies and counterstained with hematoxylin (scale bar, 200 μm). C, NAMPT expression was induced by exogenous treatment with 500 μmol/L H$_2$O$_2$ in CRC cell lines. D, Protein levels were analyzed by densitometry using the ImageJ software. E, HCT116 cells were treated with 800 μmol/L H$_2$O$_2$ or 1 mmol/L NAD$^+$ for 24 h. Cell death was assessed by trypan blue staining. F, RKO cells were treated with 800 μmol/L H$_2$O$_2$ or 1 mmol/L NAC for 24 h. Cell death was assessed by trypan blue staining. G, RKO cells were treated with 800 μmol/L H$_2$O$_2$ for 12 h. ROS measurements were performed using carboxy-H$_2$DCFDA. The bars represent the mean ± SD (n = 9). *P < 0.05 by Student's t test. a.u., arbitrary unit

during CRC progression and that imaging NADH fluorescence using TPEF microscopy could be a robust method for detecting tumor tissue in AOM/DSS mice.

3.4 | Increases in the NAS(H) pool by nicotinamide phosphoribosyltransferase protect cancer cells against detrimental oxidative stress

Azoxymethane/dextran sodium sulfate mice have been widely utilized to examine the role of inflammation in colon carcinogenesis and the contribution of inflammation-induced ROS production to CRC progression.[21] Because NAMPT has been reported to increase the antioxidant capacity of tumor cells,[15] we investigated whether the NAD(H) pool increased by NAMPT would regulate the inflammation-induced ROS levels in AOM/DSS mice. The ROS levels were significantly increased in AOM/DSS mice (Figure 4A). Interestingly, the regions of tumor tissues with high levels of NADH exhibited low levels of ROS relative to the surrounding regions

with low levels of NADH (Figure 4A). To confirm that ROS production was increased by inflammatory cytokines and immune cells in AOM/DSS mice, we detected IFN-γ and the macrophage marker F4/80 by IHC experiments. Both proteins were expressed at higher levels in CRC tissues than in normal gut tissues (Figure 4B). These results indicate that the ROS level was increased by inflammation in AOM/DSS mice and was downregulated in tumor regions with large NAD(H) pools. Our findings suggest that the increase in NAD(H) pools in tumor tissues could reduce the detrimental oxidative stress induced by inflammation.

Next, we investigated whether decreasing the excessive ROS levels by increasing the NADH pool size would promote CRC cell survival. We found that exogenous H_2O_2 treatment increased NAMPT expression by approximately 3-fold in CRC cell lines and produced only marginal changes in normal gut epithelial CCD-18Co cells (Figure 4C,D). Moreover, NAMPT knockdown and FK866 treatment dramatically increased CRC cell death and ROS levels upon H_2O_2 treatment, and this effect was rescued by treatment with
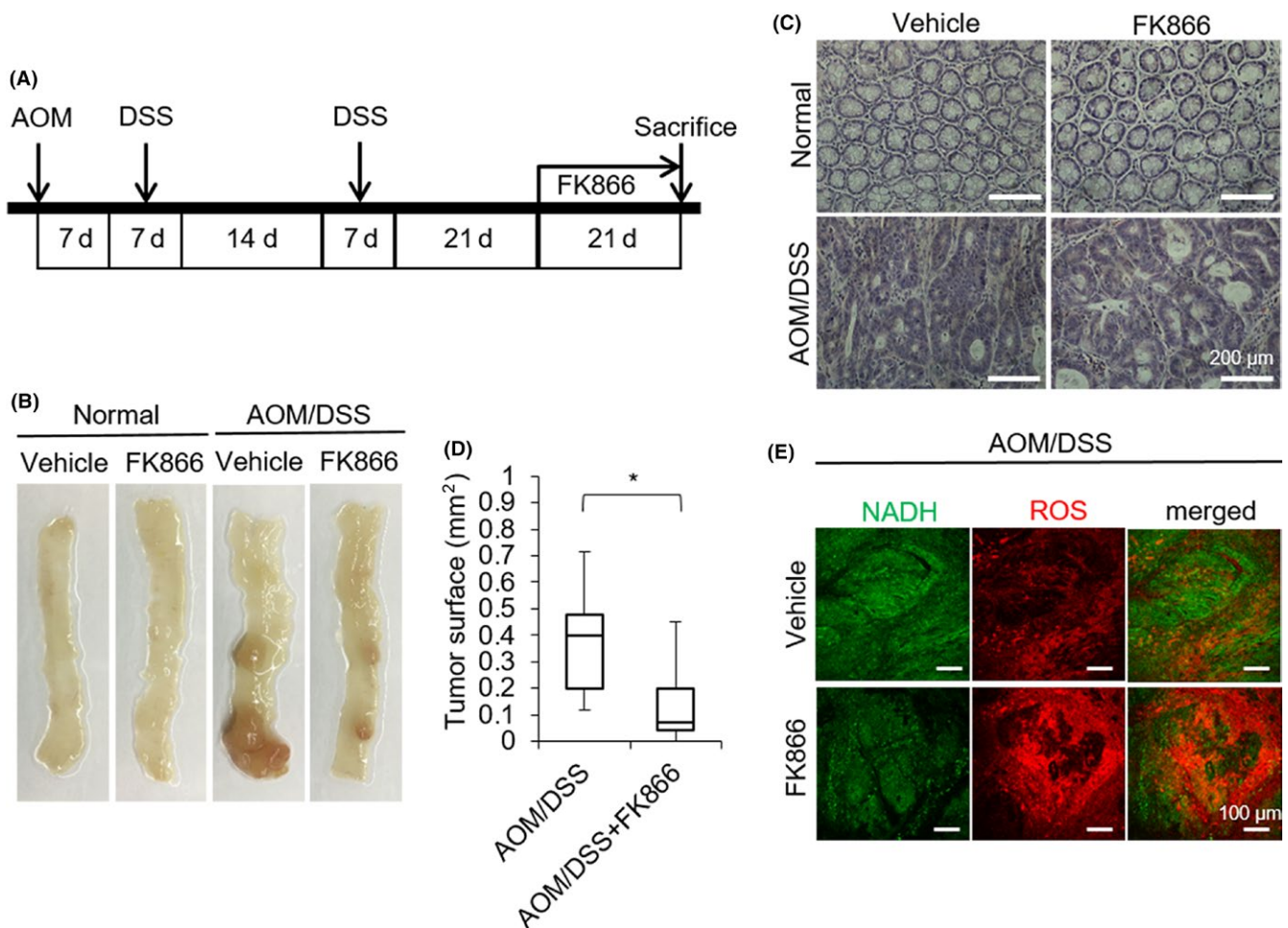

FIGURE 5 FK866 inhibited colorectal cancer (CRC) progression in azoxymethane/dextran sodium sulfate (AOM/DSS) mice. A, Experimental scheme used to administer FK866 to AOM/DSS mice. FK866 (10 mg/kg) was injected i.p. 21 d after the final DSS cycle. B, Representative images of excised mouse colon tissue. Mice were killed 21 d after the initial FK866 injection (n = 5 per time point). C, Tumor tissues were embedded in paraffin and sectioned (5 μm thick). The sections were stained with H&E (scale bar, 200 μm). D, The tumor surface size was measured. *P < .05 by Student's t test. E, The NADH fluorescence and reactive oxygen species (ROS) levels were determined by two-photon excitation fluorescence (TPEF) microscopy after incubation with carboxy-H_2DCFDA dye (scale bar, 100 μm)
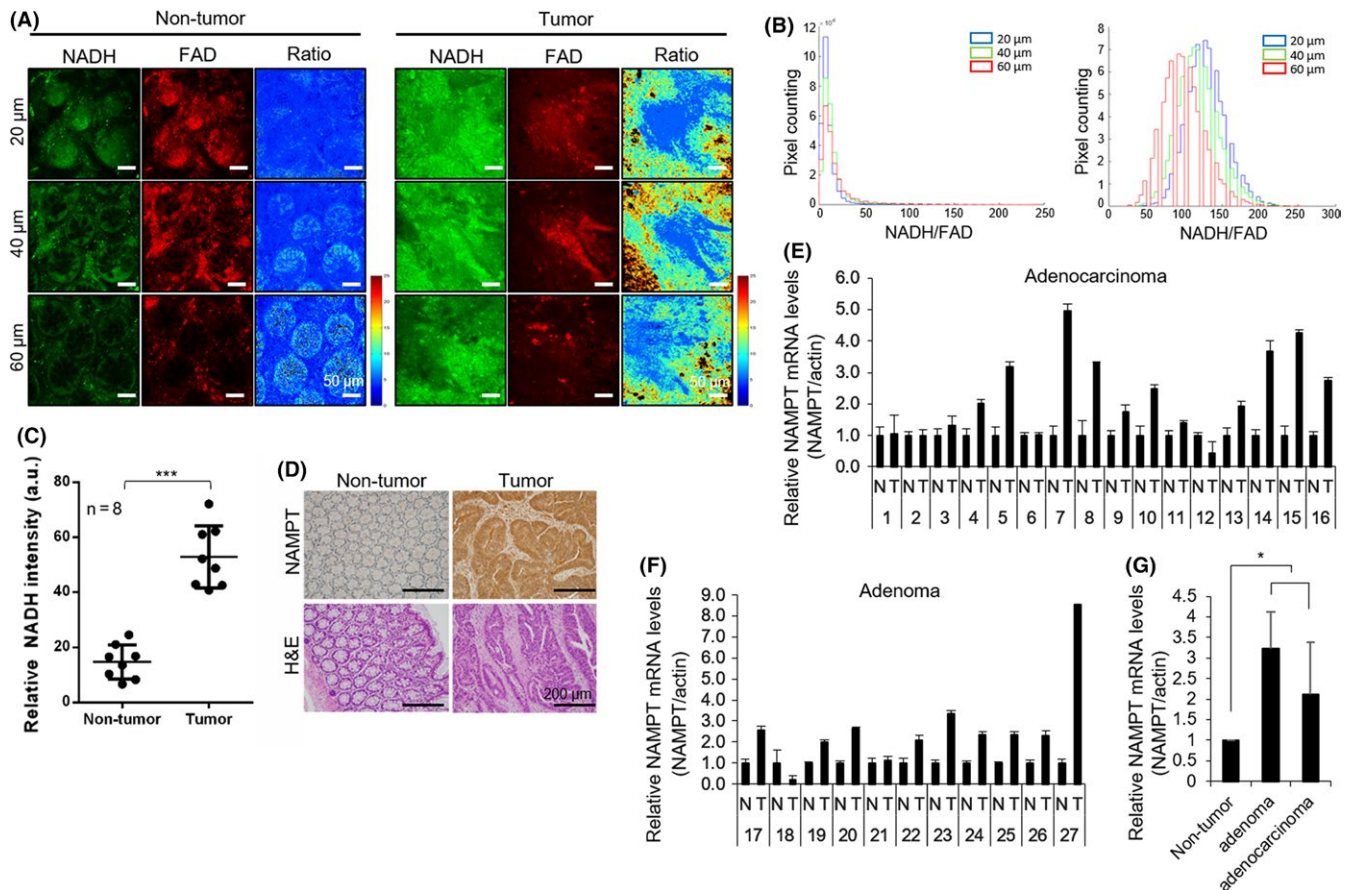
FIGURE 6 The NAD(H) pool size was increased in human colorectal tumor tissue. A, Representative images of tissues from colorectal cancer (CRC) patients. NADH and FAD fluorescence levels were detected in non-tumor and tumor tissues from CRC patients by two-photon excitation fluorescence (TPEF) microscopy (scale bar, 50 μm). B, NADH/FAD ratios were quantified using the MATLAB program. C, NADH fluorescence intensities of patient tissues at 40 μm were quantified. ***$P < .0001$ by Student's t test. D, Patient tissues were embedded in paraffin and sectioned (5 mm thick). The sections were stained with anti-nicotinamide phosphoribosyltransferase (NAMPT) antibody (upper) and H&E (down) (scale bar, 200 μm). E-G, Nicotinamide phosphoribosyltransferase (NAMPT) mRNA levels were quantified in adenocarcinoma and adenoma tissues from CRC patients by quantitative PCR

NAD$^+$ or NAC (Figure 4E-G). Collectively, these findings indicated that upregulation of NAMPT by inflammation-induced ROS production protected tumor cells against excessive oxidative stress and promoted CRC progression.

3.5 | FK866 inhibits colorectal cancer progression in azoxymethane/dextran sodium sulfate mice

To investigate whether NAMPT inhibition could suppress CRC progression in AOM/DSS mice, FK866 was i.p. injected into mice 21 days after DSS treatment (Figure 5A). We confirmed that FK866 treatment suppressed AOM/DSS-induced progression of CRC by imaging the large intestine (Figure 5B). FK866 treatment did not induce morphological changes in the gut crypt organization (Figure 5C), although the tumor surface area was reduced by FK866 (Figure 5D). FK866 treatment decreased NADH fluorescence intensity and significantly increased ROS levels in AOM/DSS mice (Figure 5E). These data indicated that FK866 could inhibit CRC progression in AOM/ DSS mice by causing excessive accumulation of ROS.

3.6 | The NAD(H) pool increases in human colorectal tumor tissue

As noted above, larger NAD(H) pools were observed in CRC cell lines and AOM/DSS mouse tissues than in normal cell lines and normal gut tissue. Therefore, we examined whether the NAD(H) pool size was also increased in tumor tissues from adenocarcinoma patients (Table S1). Similar to AOM/DSS mice, the NADH fluorescence intensity was significantly stronger in tumor tissue than in non-tumor tissue (Figures 6A,C and S3A-G). In contrast, FAD fluorescence intensity was reduced in CRC tissue compared with non-tumor tissue, leading to an increased redox ratio in CRC tissue (Figure 6B). Consistent with the NADH fluorescence intensity, NAMPT protein levels were also upregulated in tumor tissues (Figures 6D and S3A-G). Next, we confirmed that the NAMPT mRNA levels were upregulated in adenoma and adenocarcinoma tissues relative to non-tumor tissues collected from patients (Figure 6E-G and Table S2). Our data indicated that upregulated NAMPT expression could increase the NAD(H) pool size in the tumor tissues of CRC patients.

4 | DISCUSSION

Cancer cells require significantly more NAD^+ than normal cells due to their elevated metabolic needs. The cytosolic NAD^+/NADH ratio was reported to downregulate in cancer cell lines such as H1299, U87 and MDA-MB468, as observed by genetically engineered fluorescent biosensors that can measure protein-unbound species of NAD(H).[22,23] In this study, we quantified the total NAD(H) levels in whole cell lysates by enzymatic assays. Both the NAD^+/NADH ratio and NAD(H) pool size were increased according to colon cancer progression in response to enhanced NAD^+ influx due to upregulation of enzymes in NAD^+ salvage synthesis. In particular, NAMPT was critical to maintain the NAD(H) pool size and NAD^+/NADH ratio (Figure 2) and was also upregulated in colon cancer tissues of patients (Figure 6). Consistently, NAMPT expression was correlated with colon cancer patient outcome regardless of the tumor staging and induced cancer stem-like properties in colon cancer.[24] Furthermore, reduction of the NAD(H) pool by FK866 treatment effectively inhibited AOM/DSS-induced colon cancer (Figure 5), supporting that NAMPT-mediated NAD(H) pool increase could be critical to colon cancer progression. In contrast, suppression of de novo NAD^+ synthesis by unconventional pre-fold in RPB5 interactor (URI) expression is known to promote liver tumorigenesis in a diethylnitrosamine-induced hepatocellular carcinoma mouse model.[25] Therefore, it would be worthwhile to further investigate whether inhibition of salvage NAD^+ synthesis by NAMPT knockout could affect cancer progression in a mouse model.

Because NADH is autofluorescent, whereas NAD^+ is not, we examined whether NADH levels could represent the NAD(H) pool size. We confirmed that NADH levels could be positively correlated with the NAD(H) pool size and NAD(H) levels determined by enzymatic assays were also consistent with the fluorescence intensity determined by TPEF microscopy (Figures 1, 3 and 6). These results support that the fluorescence intensities detected by TPEF microscopy could represent the NAD(H) pool size. Furthermore, because NADPH and NADH are spectrally identical, we investigated the effects of NADPH levels on the fluorescence intensity using a TPEF microscope at a 740-nm wavelength. Fluorescence lifetime imaging could differentiate between NADPH and NADH because the fluorescence lifetime of cellular NADPH could be distinct from that of cellular NADH as a result of the different cofactors bound by the enzymes.[26] However, we measured the total NADH and NADPH levels, including unbound and bound forms. Decreasing the NADPH level through G6PD knockdown did not significantly affect the TPEF imaging results because the NADH levels were approximately 2-fold higher than those of NADPH (Figure S1). In addition, the NADPH level should also sustain cancer cell resistance to detrimental oxidative stress because NADPH is an antioxidant molecule. Thus, imaging by TPEF microscopy at a 740-nm wavelength could indicate the resistance to therapies that can induce oxidative stress. Furthermore, Wang et al[27] showed the typical glandular structures of normal mouse colon by TPEF endoscopy as well. Therefore, NADH imaging by TPEF endoscopy could be a potential strategy for CRC diagnosis.

Reactive oxygen species can act as anti-tumorigenic agents, depending on the cell and tissue types, the location of ROS production, the individual ROS levels and the antioxidant capacity of cancer cells.[28] Cancer cells that survive despite oxidative stress are likely to have acquired adaptive mechanisms to counteract the potential toxic effects of elevated ROS.[10] In a previous study, we reported that NAMPT could increase the antioxidant capacity of cancer cells and induce cancer cell survival under excessive oxidative stress upon glucose deprivation.[15] Consistently, NAMPT expression was not induced by H_2O_2 treatment in normal cells, but it was dramatically increased in CRC cells (Figure 4C), indicating that NAMPT expression in tumor tissues could be increased due to inflammation-induced ROS production. In tissues of CRC patients, both mRNA and protein levels of NAMPT were also upregulated (Figure 6F-I). Interestingly, tumor tissues with high levels of NADH fluorescence exhibited decreased ROS levels relative to surrounding tissues with low levels of NADH (Figure 4A). Moreover, FK866 treatment decreased the NAD(H) pool size, increased detrimental ROS levels and reduced the colon tumor size in AOM/DSS mice (Figure 5). Therefore, our results support that NAMPT-mediated NAD(H) pool increase could promote colon cancer progression by decreasing detrimental oxidative stress.

Interestingly, NAMPT was upregulated in both cancer and inflammatory immune cells (Figure S2). A previous report revealed that immune cells recruited into DSS-induced colitis tissues, such as macrophages, dendritic cells, T cells and natural killer cells, exhibited upregulated NAMPT expression, and FK866 treatment decreased inflammatory responses.[16] Consistently, the IFN-γ levels were reduced in FK866-treated AOM/DSS tissues (Figure S4). Taken together, the increases in the NAD(H) pool mediated by NAMPT could suppress excessive oxidative stress-induced cell death in cancer cells and promote inflammatory cytokine production in immune cells, leading to inflammation-induced CRC progression. Therefore, FK866 treatment increased detrimental ROS levels in cancer cells and decreased inflammatory cytokine levels in immune cells, inhibiting colon cancer progression.

In conclusion, we investigated the correlation between the NAD(H) pool size and CRC progression with its clinical implications. We confirmed that the NAD(H) pool size and NAD^+/NADH ratio could increase during CRC progression due to the increasing influx of NAD^+, which was mediated by NAMPT. NAMPT-mediated increases in the NAD(H) pool size should promote inflammation-induced CRC progression by decreasing the detrimental effects associated with excessive ROS accumulation. Furthermore, NADH might serve as a useful non-invasive marker with intrinsic autofluorescence properties because its levels could represent the NAD(H) pool size. Based on our findings, the non-invasive detection of NADH by TPEF microscopy could offer a novel imaging method for CRC progression.

DISCLOSURE

The authors declare that they have no conflicts of interest related to the contents of this article.

ORCID

Kwan Y. Choi 🆔 https://orcid.org/0000-0002-3930-3856

REFERENCES

1. Jemal A, Bray F, Center MM, Ferlay J, Ward E, Forman D. Global cancer statistics. *CA Cancer J Clin*. 2011;61:69-90.
2. Janakiram NB, Rao CV. The role of inflammation in colon cancer. *Adv Exp Med Biol*. 2014;816:25-52.
3. Ekbom A, Helmick C, Zack M, Adami HO. Ulcerative colitis and colorectal cancer. A population-based study. *N Engl J Med*. 1990;323:1228-1233.
4. Gillen CD, Walmsley RS, Prior P, Andrews HA, Allan RN. Ulcerative colitis and Crohn's disease: a comparison of the colorectal cancer risk in extensive colitis. *Gut*. 1994;35:1590-1592.
5. Ferrone C, Dranoff G. Dual roles for immunity in gastrointestinal cancers. *J Clin Oncol*. 2010;28:4045-4051.
6. Ekbom A. Risk of cancer in ulcerative colitis. *J Gastrointest Surg*. 1998;2:312-313.
7. Grivennikov SI, Greten FR, Karin M. Immunity, inflammation, and cancer. *Cell*. 2010;140:883-899.
8. Liou GY, Storz P. Reactive oxygen species in cancer. *Free Radic Res*. 2010;44:479-496.
9. Sena LA, Chandel NS. Physiological roles of mitochondrial reactive oxygen species. *Mol Cell*. 2012;48:158-167.
10. Trachootham D, Alexandre J, Huang P. Targeting cancer cells by ROS-mediated mechanisms: a radical therapeutic approach? *Nat Rev Drug Discov*. 2009;8:579-591.
11. Galli M, Van Gool F, Rongvaux A, Andris F, Leo O. The nicotinamide phosphoribosyltransferase: a molecular link between metabolism, inflammation, and cancer. *Cancer Res*. 2010;70:8-11.
12. Chiarugi A, Dolle C, Felici R, Ziegler M. The NAD metabolome–a key determinant of cancer cell biology. *Nat Rev Cancer*. 2012;12:741-752.
13. Garten A, Petzold S, Korner A, Imai S, Kiess W. Nampt: linking NAD biology, metabolism and cancer. *Trends Endocrinol Metab*. 2009;20:130-138.
14. Yang H, Yang T, Baur JA, et al. Nutrient-sensitive mitochondrial NAD$^+$ levels dictate cell survival. *Cell*. 2007;130:1095-1107.
15. Hong SM, Park CW, Kim SW, et al. NAMPT suppresses glucose deprivation-induced oxidative stress by increasing NADPH levels in breast cancer. *Oncogene*. 2016;35:3544-3554.
16. Gerner RR, Klepsch V, Macheiner S, et al. NAD metabolism fuels human and mouse intestinal inflammation. *Gut*. 2017;67:1813-1823.
17. Mujat C, Greiner C, Baldwin A, et al. Endogenous optical biomarkers of normal and human papillomavirus immortalized epithelial cells. *Int J Cancer*. 2008;122:363-371.
18. Ostrander JH, McMahon CM, Lem S, et al. Optical redox ratio differentiates breast cancer cell lines based on estrogen receptor status. *Cancer Res*. 2010;70:4759-4766.
19. Varone A, Xylas J, Quinn KP, et al. Endogenous two-photon fluorescence imaging elucidates metabolic changes related to enhanced glycolysis and glutamine consumption in precancerous epithelial tissues. *Cancer Res*. 2014;74:3067-3075.
20. Levitt JM, McLaughlin-Drubin ME, Munger K, Georgakoudi I. Automated biochemical, morphological, and organizational assessment of precancerous changes from endogenous two-photon fluorescence images. *PLoS ONE*. 2011;6:e24765.
21. De Robertis M, Massi E, Poeta ML, et al. The AOM/DSS murine model for the study of colon carcinogenesis: from pathways to diagnosis and therapy studies. *J Carcinog*. 2011;10:9.
22. Zhao Y, Hu Q, Cheng F, et al. SoNar, a highly responsive NAD+/NADH sensor, allows high-throughput metabolic screening of antitumor agents. *Cell Metab*. 2015;21:777-789.
23. Hung YP, Albeck JG, Tantama M, Yellen G. Imaging cytosolic NADH-NAD(+) redox state with a genetically encoded fluorescent biosensor. *Cell Metab*. 2011;14:545-554.
24. Lucena-Cacace A, Otero-Albiol D, Jimenez-Garcia MP, Munoz-Galvan S, Carnero A. NAMPT is a potent oncogene in colon cancer progression that modulates cancer stem cell properties and resistance to therapy through Sirt1 and PARP. *Clin Cancer Res*. 2018;24:1202-1215.
25. Tummala KS, Gomes AL, Yilmaz M, et al. Inhibition of de novo NAD(+) synthesis by oncogenic URI causes liver tumorigenesis through DNA damage. *Cancer Cell*. 2014;26:826-839.
26. Blacker TS, Mann ZF, Gale JE, et al. Separating NADH and NADPH fluorescence in live cells and tissues using FLIM. *Nat Commun*. 2014;5:3936.
27. Wang T, Li Q, Xiao P, et al. Gradient index lens based combined two-photon microscopy and optical coherence tomography. *Opt Express*. 2014;22:12962-12970.
28. Reuter S, Gupta SC, Chaturvedi MM, Aggarwal BB. Oxidative stress, inflammation, and cancer: how are they linked? *Free Radic Biol Med*. 2010;49:1603-1616.

SUPPORTING INFORMATION

Additional supporting information may be found online in the Supporting Information section at the end of the article.